Effects of Brominating Matrimid Polyimide on the Physical and Gas Transport Properties of Derived Carbon Membranes

Youchang Xiao,[†] Ying Dai,[‡] Tai-Shung Chung,*[,†] and Michael D. Guiver[‡]

Department of Chemical & Biomolecular Engineering, National University of Singapore, Singapore 117602, and Institute for Chemical Process and Environmental Technology, National Research Council of Canada, Ottawa, Ontario K1A 0R6, Canada

Received June 25, 2005; Revised Manuscript Received September 12, 2005

ABSTRACT: Bromination modification was initially carried out on Matrimid polyimide before undergoing carbonation to produce carbon membranes. Compared with unmodified Matrimid, brominated Matrimid shows lower chain flexibility, which is demonstrated by increased glass transition temperatures and molecular simulation results. Additionally, an increase in space between polymer chains was supported by fractional free volume (FFV) and *d*-spacing measurements. The improvement of chain rigidity of polyimide precursors serves to strengthen the membrane morphology during the production of carbon membranes. Thermal gravimetric analysis indicates that the thermal stability of polyimide decreases after bromination. The lower thermal stability and higher FFV value of brominated Matrimid result in higher gas permeability of carbon membranes pyrolyzed at a low pyrolysis temperature, while the selectivity remained competitive to those pyrolyzed from the original Matrimid precursor under the same conditions. However, the gas permeabilities of carbon membranes derived from modified Matrimid decrease significantly and become lower than those of carbon membranes from the original Matrimid, when the pyrolysis temperature is raised to 800 °C. This is due to the formation of more graphitic-like structure in carbon membranes from brominated polyimide, observed by the wide-angle X-ray diffraction. Therefore, it is concluded that bromination of Matrimid polyimide has significantly affected the pyrolysis behavior and the structure of the resulting carbon membranes. At a low pyrolysis temperature, carbon membranes derived from brominated precursors show attractive and superior gas separation performance.

1. Introduction

Membrane technology offers an alternative to traditional separation processes for gas separations such as air separation, natural gas production, olefin/paraffin separation, and hydrogen recovery,[1−4] due to its lower cost, smaller size, higher energy savings, and better environmental benefits. Among the various membrane materials, carbon membranes show numerous advantages[5,6] such as (1) consisting of ultra-micropores with similar sizes to the dimensions of gas molecules and showing excellent gas separation performance, (2) exhibiting high thermal stability, mechanical strength, and chemical resistance, and (3) having gas permeation properties less influenced by the feed pressures and also time independent.

Carbon membranes are typically prepared by the pyrolysis of thermosetting polymeric precursors, which do not fuse and retain their membrane shape during carbonization. The gas separation performance of carbon membranes largely depends on the chemical structures of polymeric precursors, membrane formation methods, pyrolysis conditions, and posttreatment methods. Although great efforts have been made to understand the processes involved in developing high-performance carbon membranes, most work still relies on empirical methods to prepare carbon membranes because of the complexity of the structure formation during carbonization of the polymers. One of the most important factors determining the separation performance of carbon membranes is the choice of polymeric precursors. The polymeric precursors reported include poly(furfuryl alcohol) (PFA),[7] poly(vinylidene chloride) (PVDC),[8,9] cellulose,[10,11] phenolic resins,[12,13] polyacrylonitrile (PAN),[14] poly(ether imide)s,[15,16] and polyimides.[17−27] Among these polymers, aromatic polyimides are the most frequently utilized for the preparation of carbon membranes without support because this class of polymers has a rigid structure, with high glass transition temperatures (T_g) and excellent thermal stability. Koros et al. reported hollow fiber carbon membranes derived from a copolyimide (BPDA/6FDA-TrMPD), which exhibited an O_2 permeance of 15−40 GPU and a separation factor of 11−14.[22] Kusuki et al. developed a manufacturing method to continuously prepare hollow fiber carbon membranes using polyimide as the precursor.[23] Okamoto et al. reported excellent performance for olefin/paraffin separation with carbonized hollow fiber membranes derived from BPDA−DDBT/BADA copolyimide.[24] After a comparison with a series of carbon membranes pyrolyzed from four polyimides (DAI/6FDA, DAI/BTDA, DAI/BPDA, and DAI/ODPA) synthesized from different dianhydrides, Xiao et al. concluded that higher FFV and lower thermal stability of polyimide precursors led to higher gas permeability of carbon membranes at a mild pyrolysis temperature (550 °C). When polyimides were carbonized at a high temperature (800 °C), better chain flatness and in-plane orientation of polyimides contribute to higher gas selectivity in carbon membranes, due to the formation of more graphitic-like structure during carbonization.[27]

However, most of the polyimides for carbon membrane studies are only synthesized on the laboratory scale. From a practical point of view, the high cost of synthesized polyimides is a key factor that limits their utilization in the preparation of carbon membranes.

[†] National University of Singapore.
[‡] National Research Council of Canada.
* Corresponding author: e-mail chencts@nus.edu.sg, Fax (65)-67791936.

10.1021/ma051354j CCC: $30.25
Published on Web 11/05/2005

Therefore, the selection of commercially available polyimides such as Kapton, Matrimid, and P84 as precursors would be the preferred route for the development of carbon membranes.[17−20] Once a suitable polyimide precursor is identified, the carbonization conditions must be elaborated in order to obtain carbon membranes with desirable performance. Geiszler and Koros[28] reported that the pyrolysis conditions, such as pyrolysis temperature, heating rate, and pyrolysis environments, appreciably affect the properties of resultant carbon membranes. On the other hand, the pretreatment of polyimide precursors can also play an important role to improve separation performance of resultant carbon membranes. Kusuki et al.[25] and Okamoto et al.[26] thermally treated the polyimide precursors in air before pyrolysis to strengthen the structure of precursors. As a result, the polyimide can maintain good membrane morphology after the high-temperature pyrolysis. Tin et al.[18,19] developed another two modifications based on (1) chemical cross-linking and (2) alcohol pretreatment on polyimide precursors. These two modifications introduced small molecules between polyimide chains before pyrolysis. The space-filling effects of these small molecules were considered as the main reason for the enhanced performance of resultant carbon membranes.

Bromination of polymer is a widely used modification method to enhance the separation performance of polymeric membranes. McCaig et al. have reported that glassy polymers with bromine substitution on the aromatic rings exhibited superior gas separation relative to their structure analogues containing no bromine atoms, since the bromine atoms contribute to the steric hindrance of torsional rotations about the phenyl ring and polar interacts with certain gas penetrants.[29] Bromination of PPO was studied by Percec et al.[30] and Hamad et al.[31] They concluded that a high degree bromination of PPO decreased the flexibility of the polymer chains which was evidenced by an increase in the T_g. Bromine atoms were first introduced into polyimides by Okamoto et al.[32] and Liou et al.[33] using the free-radical bromination of alkyl groups and the polymerization of halogen-containing monomers. The brominated polyimides were prepared for two purposes: to improve solubility by a reduction in chain packing and crystallinity as well as to increase reactivity by the substitution of bromine with other useful functionalities for applications in pervaporation and photorefractive materials. After Guiver et al. reported the preparation of modified Matrimid polyimide by electrophilic bromination,[34] it is possible to directly brominate commercial polyimides. On the basis of our previous study,[27] polyimides with more rigid chains, structural planarity, higher FFV, and lower thermal stability are preferred as candidates for carbon membrane precursors.

In this study, bromination was considered as a pretreatment of commercial polyimide precursors to prepare carbon membranes for the first time. Bromine atoms bonded to polyimide chains are expected to increase the polymer chain rigidity. Therefore, the structure of precursors should be strengthened and membrane morphology should be better maintained during pyrolysis. Additionally, bromine atoms may inhibit the chain packing and decompose at relatively lower temperatures with the loss of Br_2 or HBr. This effect is equivalent to an increase of the free volume in the matrix, resulting in more and bigger pore structures in resultant carbon membranes.

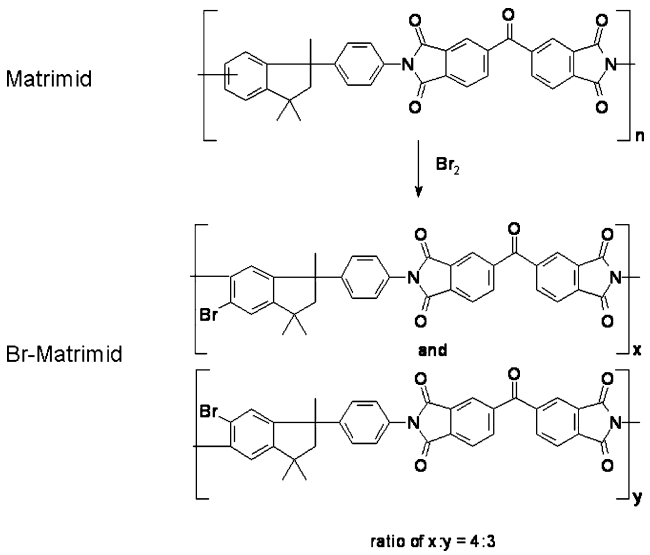

Figure 1. Reaction Scheme for the bromination of Matrimid.

The aim of this study is also to explore a method of tailoring micropores in the preparation of carbon membranes by introducing a decomposable group such as bromine atoms into commercial polyimides in an effort to understand the factors determining the micropore formation during the pyrolysis of polyimides. Thermal properties of brominated polyimide were tested by differential scanning calorimetry (DSC) and thermal gravimetric analysis (TGA). Simple simulation was used to characterize the conformational differences between the original polyimide and brominated polyimide. The heat treatment and carbonization of brominated polyimide were monitored by TGA-FTIR, FTIR-ATR, and XPS. The structure of resultant carbon membranes was discussed on the basis of X-ray diffraction and the permeation behaviors of pure gases such as O_2, N_2, CO_2, and CH_4.

2. Experimental Section

2.1. Materials. A commercially available polyimide-type polyimide was selected as a precursor in this study, which was a BTDA−AAPTMI polyimide (Matrimid 5218, Ciba Specialty Chemicals). The chemical structure is shown in Figure 1. The bromine-modified polymers were prepared with bromine and chloroform as received. Dichloromethane was used as the solvent for polyimides to prepare the dense films.

2.2. Preparation of Brominated Matrimid 5218. Brominated Matrimid (Br-Matrimid) was prepared as shown in Figure 1. Details of the synthetic procedures and structural analyses were published by Guiver et al.[34] The bromination was conducted by the reaction of bromine with a chloroform solution of Matrimid polyimide over a period of 6 h. Methanol was used to precipitate the resulting Br-Matrimid and extract unreacted free bromine. The Br-Matrimid polyimide was purified by redissolution and precipitation, followed by vacuum-drying. Elemental analyses indicated that a total substitution of slightly more than one bromine per repeat unit occurred, when the addition of bromine is in excess of 1 mol in relation to polyimide units.

2.3. Preparation of Polyimide Precursor Membranes. Before pyrolysis, polyimide precursors were first prepared as dense films. Dilute solutions of less than 2 wt % polyimides in dichloromethane were prepared and filtered using 1 μm filters to remove undissolved materials and dust particles. The solution was then cast on a leveled clean silicon wafer at room temperature. The polymer films were formed after most of the solvent had evaporated slowly. The nascent films were dried in a vacuum at 250 °C for 48 h to remove any residual solvent.

Membranes films with a thickness of about 50 μm were chosen for testing and pyrolysis.

2.4. Preparation of Carbon Membranes. The pyrolyses were performed using a Centurion Neytech Qex vacuum furnace. Pyrolyses temperatures from 400 to 800 °C were used in the preparation of carbon membranes for this study. In general, the final pyrolysis temperature was attained in several steps: the polymer films were heated to 250 °C from room temperature at a rate of 10 °C/min; subsequently, the temperature was raised to a set value at a very slow rate of 0.2 °C/min to prevent cracking of carbon membranes. Finally, it was held isothermally at the final temperature for 2 h. After completing the pyrolysis process, membranes were cooled slowly at 1 °C/min in the vacuum furnace to room temperature and stored in a drybox for further studies.

2.5. Characterization of Membranes. In a nitrogen environment with a heating rate of 10 °C/min, the thermal properties of polyimides were monitored by DSC using a Shimadzu 40 type instrument and by TGA using a Perkin-Elmer thermal gravimetric analyzer. With the aid of N_2 flow, the exhaust products from TGA were flushed through a transfer line to a gas cell of a Bio-Rad FTS 3500 FTIR spectrometer. The temperature of the transfer line and gas cell was set at 150 °C to prevent condensation of gas products. With TGA-FTIR, the mass loss throughout the profiles and materials evolved at particular temperature can be obtained.

The chain properties of polyimides also were simulated by Cerius[2] software using a SGI (Silicon Graphic Inc.) workstation. Since the molecular weight of Matrimid and Br-Matrimid is around 50 000−60 000 as measured by GPC (gel permeation chromatography), which corresponds approximately to 100 repeating units, each polyimide chain was built by the random polymer builder with 100 repeating units so that the system size is adequate to represent the conformation of a real polymer chain. The initial structure of polyimide chain was first optimized by a molecular mechanics technique. Then a RMMC (the "RIS" Metropolis Monte Carlo method) module within the Cerius[2] for material science was used to calculate the properties of polymer chains at 300 K, such as the mean-squared end-to-end distance, molar stiffness function, and intrinsic viscosity of the polymer chains.[35] The most advanced polymeric force field, pcff (polymer consistent force field), was used for all systems. In addition, van der Waals interactions, electrostatic (Coulombic), and torsion interactions were included in RMMC simulation. During calculations, 100 000 steps were used in the equilibrium portion while 500 000 steps were used in the production portion of the "RIS" Metropolis Monte Carlo simulation. Ten conformations of polymer chain were built for the particular polyimide, and the results were averaged from these calculations.

An X-ray photoelectron spectrometer was utilized to measure elemental ratios and monitor the chemical change on the film surface during pyrolysis. The XPS measurements were carried out by an AXIS HSi spectrometer (Kratos Analytical Ltd., England) using a monochromatic Al Kα X-ray source (1486.6 eV photons) at a constant dwell time of 100 ms and a pass energy of 40 eV. The anode voltage and anode current were 15 kV and 10 mA, respectively. The pressure in the analysis chamber was maintained at 5.0×10^{-8} Torr or lower during each measurement. All core-level spectra were obtained at a photoelectron takeoff angle of 90° with respect to the sample. FTIR-ATR (Fourier transformed infrared spectroscopy−attenuated total reflection model) was also carried out using a Perkin-Elmer FTIR microscope at 8 cm^{-1} resolution over the 500−2200 cm^{-1} range. Each sample was scanned 20 times.

Wide-angle X-ray diffraction (WAXD) was performed using a Bruker X-ray diffractometer at room temperature with Cu Kα radiation of wavelength 1.54 Å. The d-spacing can be calculated from Bragg's rule as follows: $n\lambda = 2d \sin \theta$, where d is the dimension spacing, θ is the diffraction angle, λ is the X-ray wavelength, and n is an integral number (1, 2, 3, ...).

The pure gas permeabilities (in barrers, 1 barrer = 1×10^{-10} cm^3 (STP) cm/(cm^2 s cmHg)) of O_2, N_2, CO_2, and CH_4 were measured using the standard constant-volume method. The testing temperature and pressure was 35 °C and 10 atm, respectively. The details of apparatus design and testing procedures have been reported elsewhere.[36] The ideal selectivity is determined from $\alpha_{A/B} = P_A/P_B$.

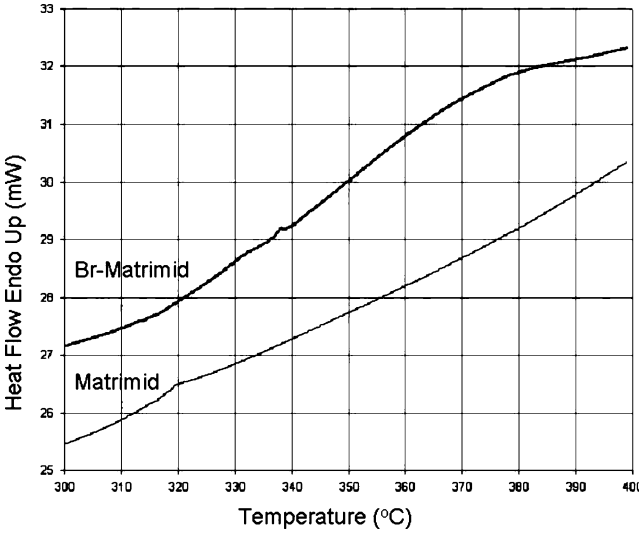

Figure 2. DSC of Matrimid and brominated Matrimid PI.

3. Results and Discussion

3.1. Effects of Bromination on the Thermal Properties of Matrimid PI. The T_g's of Matrimid and Br-Matrimid were determined from DSC measurements, as shown in Figure 2. Compared with the heat flow curve of Matrimid, there is a very broad endothermal peak from 320 °C during the heating run of the Br-Matrimid. This may be attributed to the degradation of brominated polymer. However, the T_g can still be observed. In the case of Matrimid, T_g increases from 320 to 338 °C after bromination, resulting from hindered rotation from the bulky bromine atoms. This is evidence of an increase in polymer chain stiffness, also supporting by RMMC simulation. Table 1 lists selected simulated properties, which are the mean-squared end-to-end distance, molar stiffness, intrinsic viscosity, and dihedral angle between imide and aromatic ring, of Matrimid and Br-Matrimid with same number of repeat units. After bromination, the mean-squared end-to-end distance, molar stiffness, and intrinsic viscosity of Matrimid polyimide all increase by almost a half value, indicating better linearity and rigidity of Br-Matrimid chains. Molar stiffness expresses the molecular mobility of polymer chains quantitatively and was calculated from mean square of end-to-end distance obtained from the computer simulation.

Figure 3 shows the TGA-FTIR analysis of Matrimid and Br-Matrimid polyimides. In Figure 3, the X axis represents the temperature and the Y axis represents the weight percent for TGA and the wavenumbers for FTIR spectra. The thermal stability of polyimides was indicated by TGA curves and the composition of released gases during the thermal decomposition of polyimides was analyzed by FTIR spectra. The understanding of the thermal decomposition and the evolving gas composition of precursors at different temperatures is instructive in realizing the possible structures of corresponding carbon membranes under different pyrolysis conditions. The decomposition of Matrimid polyimide occurs at a temperature of around 500 °C, and the most rapid rate of weight loss takes place at around 520 °C. After bromination, the first weight loss of Br-Matrimid

Table 1. Physical Properties of Polyimides Simulated by RMMC Module in Cerius²

	mean squared end-to-end distance (Å²)	molar stiffness function ($g^{0.25}cm^{1.5}/mol^{0.75}$)	intrinsic viscosity (cm^3/g)	dihedral angle between imide−aromatic rings (deg)
Matrimid	$(6.3 \pm 0.8) \times 10^4$	306	71.95	50.4
Br-Matrimid	$(9.4 \pm 1.2) \times 10^4$	425	113.8	50.4

occurs around 300 °C, about 200 °C lower than that of Matrimid, and the most rapid rate of Br-Matrimid decomposition takes place at around 490 °C, indicating lower thermal stability of Br-Matrimid compared with Matrimid polyimide. As the temperature increases, both polyimides show a second decomposition peak at 600 °C. Lower thermal stability of Br-Matrimid may be the result of Br−C bond cleavage at lower temperatures. In addition, the evolution of Br from polyimide chains may produce free radicals, which accelerate the decomposition of polyimide, resulting in the forward movement of the decomposition peak of Br-Matrimid.

The following characteristic bands can be observed in FTIR spectra of evolution gases during the pyrolysis: CO_2 at the characteristic band around 2350 cm^{-1}, CO at its characteristic double bands (2170 and 2110 cm^{-1}), hydrocarbons C−H at the characteristic bands around 3050 and 1390 cm^{-1}, and unsaturated C=C at the characteristic bands around 1650 cm^{-1}. The majority of hydrocarbons produced during Br-Matrimid pyrolysis releases at around 350 °C, while the release of hydrocarbons only occurs at around 520 °C during Matrimid pyrolysis. However, few CO_2 and CO bands are detected when Br-Matrimid is pyrolyzed at 350 °C, and most of these two gases were still released at 500 °C as occurred with the Matrimid pyrolysis process. A possible reason is that the evolution of hydrocarbons mainly comes from decomposition of the indan groups in the Matrimid structure. The decomposition of indan groups is activated by the free radical produced during the pyrolytic release of Br atoms, which are in close proximity to the indan groups. The released CO_2 and CO arise mainly from the imide groups, which are only decomposed at temperatures of around 500 °C. Since the decomposition of imide groups is also elicited by radicals, the fastest rate of weight loss during polyimide pyrolysis may occur much earlier if Matrimid is brominated.

3.2. Chemical Changes of Brominated Matrimid Polyimide during Pyrolysis. The chemical changes of Br-Matrimid during pyrolysis were monitored by ATR-FTIR and XPS. Although these two characterization methods are restricted to probing near the surface of membranes, the results are assumed to represent the chemical changes throughout the whole membranes. Figure 4 shows ATR-FTIR spectra of the Br-Matrimid polyimide and resultant carbon membranes pyrolyzed under different pyrolysis temperatures. The intensities of the peaks assigned to a symmetric C=O stretch (1776 cm^{-1}), asymmetric C=O stretch (1720 cm^{-1}), C−N stretch (1353 cm^{-1}), and bending of C=O (741 cm^{-1}) are constant when the membranes are thermally treated at 400 °C for 2 h. This result indicates that the imide groups of Br-Matrimid are stable at 400 °C and is consistent with the fact that the decomposition of Br may not have a significant influence on the imide groups in the Br-Matrimid polyimide when the pyrolysis temperature is below 500 °C.

Once a pyrolysis temperature of 500 °C is attained, the intensities of peaks representing imide groups are reduced. For the membranes pyrolyzed at 600 °C, the absorbances of these bands almost disappear, indicating that the imide ring was decomposed completely at this temperature. On the other hand, the absorption bands around 2900−3000 cm^{-1}, which are assigned to alkyl of indan groups, are observed in the sample of Br-Matrimid heat-treated at 250 °C. After thermal treatment at 400 °C, these bands are not observed. This phenomenon provides evidence that the indan groups of brominated Matrimid decompose at around 400 °C.

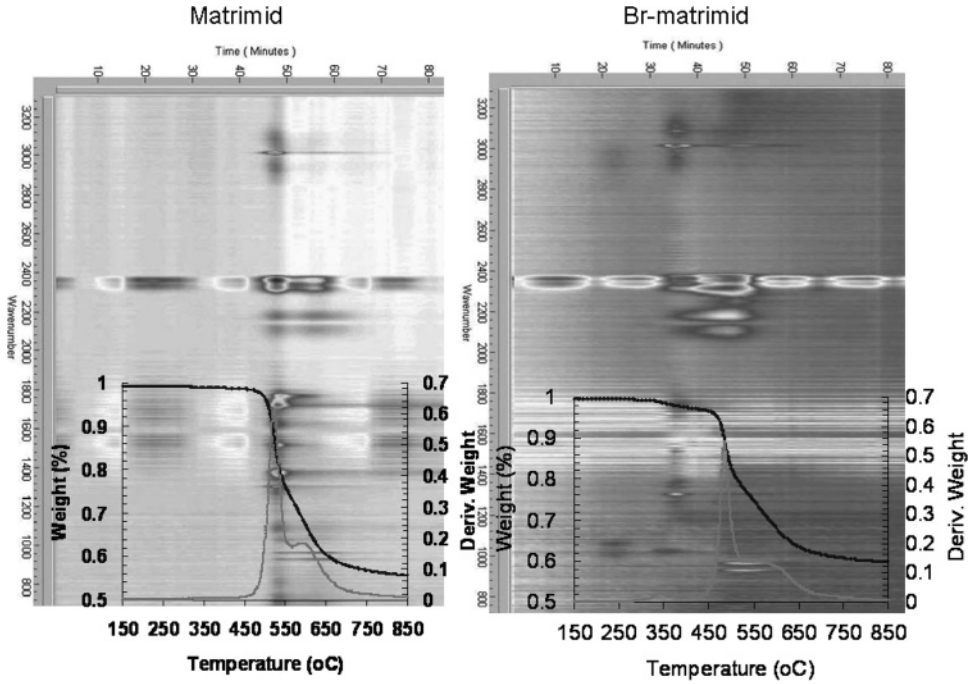

Figure 3. TGA-FTIR of Matrimid and brominated Matrimid.

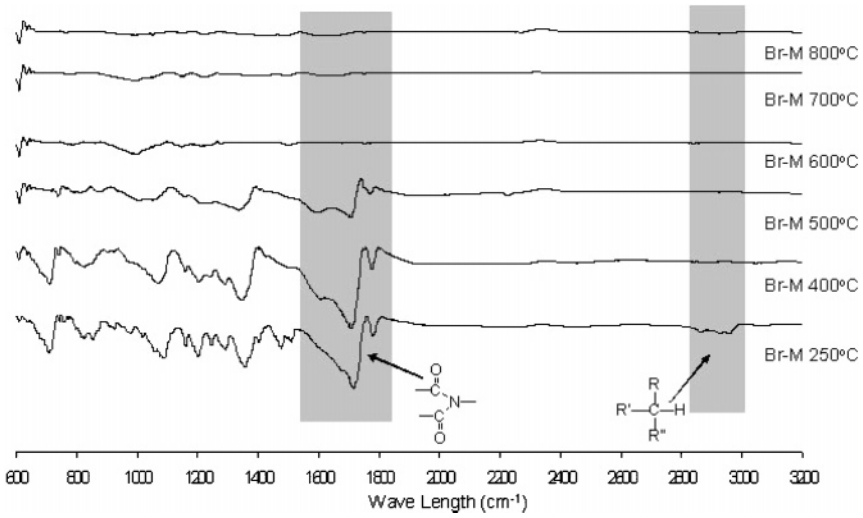

Figure 4. FTIR-ATR spectra of brominated Matrimid film after different pyrolysis temperatures.

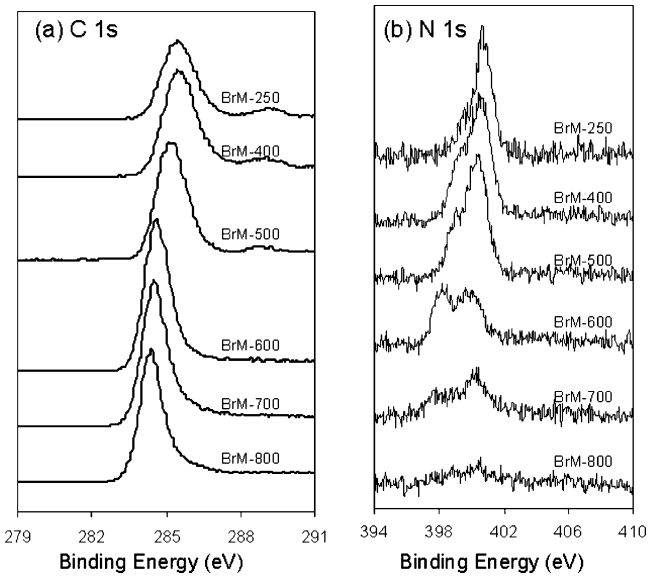

Figure 5. Changes in XPS spectra of carbon membranes from brominated Matrimid under different pyrolysis temperatures.

When the pyrolysis temperature is further increased to 600−800 °C, most peaks attributed to organic groups disappeared, suggesting that polymer is fully carbonized at such temperatures.

The variations of C 1s and N 1s XPS spectra with carbonization temperature up to 800 °C are shown in Figure 5a,b. In Figure 5a, the Br-Matrimid precursor has two peaks in the C 1s spectrum, which are a broad strong one around 284−286 eV and a weak one at around 289 eV. This broad strong peak is attributed to the combination of C−H species and C−N species in the molecular structure of Br-Matrimid. It becomes sharper and moves to lower binding energy direction with an increase in carbonization temperature. The binding energy value finally settles near 284.5 eV after 2 h heating at 800 °C. The binding energy of 284.5 eV agrees with that reported for graphite, indicating that some graphite-like carbon structures are formed from polyimide precursors after pyrolysis at 800 °C.[37] The peak around 289 eV for the original Br-Matrimid is assigned to carbonyl in the imide structure. This peak keeps constant after heat treatment at 400 °C and becomes weak with increasing pyrolysis temperature and gradually disappears when the temperature is above 600 °C. The change agrees with previous TGA-FTIR and FTIR-ATR results that imide groups are stable at 400 °C and are decomposed above the 500 °C.

As shown in Figure 5b, the peak of N 1s electrons for the original Br-Matrimid is located at around 401 eV. The position of this peak remains almost constant with the thermal treatment but shows a small shoulder at a lower binding energy side. The shoulder may arise from the cleavage of C−N bonds between imide groups and brominated phenyl rings induced by the release of bromine atoms. Moreover, the shoulder continues a shift to lower binding energy and becomes a new peak located at 398 eV at 600 °C. This new peak may be the result of C═N− or C≡N groups formed during the decomposition of imide groups. This phenomenon implies that the intermediate state of nitrogen in carbon membranes pyrolyzed below 600 °C may be assigned to pyridine-type nitrogen. When the pyrolysis temperature increases to 700 °C, the relative intensity of the peak at 398 eV decreased gradually, indicating that the double or triple bonds between C and N revert to a single bond. At this temperature, the state of nitrogen in the resultant carbon membranes can be described as pyrrole-type nitrogen.[37] When the pyrolysis temperature is increased to 800 °C, the intensity of N 1s spectrum becomes extremely weak, showing that most N atoms near the surface of the membrane have been driven off during the carbonization process.

Figure 6 shows the WAXD results for Br-Matrimid polyimide and its derived carbon membranes at different pyrolysis temperatures. WAXD is a useful technique for measuring the difference in interlayer spacing between polymer chains and carbon materials. When heating temperature is below 500 °C, the X-ray diffractions show a very broad peak from 15° to 30°, indicating the amorphous structure of brominated polyimide. When heating temperature is increased beyond 500 °C, the broad peak becomes sharper and moves to a larger θ angle direction. This means that an ordered structure is gradually constructed in the matrix and that the distance between chains becomes smaller during the pyrolysis process. A new peak at $2\theta = 43°$ is obviously observed in carbon membranes pyrolyzed at temperatures higher than 700 °C, and its intensity becomes stronger with an increase in temperature. This peak could be pointed to the graphite (100) plane which

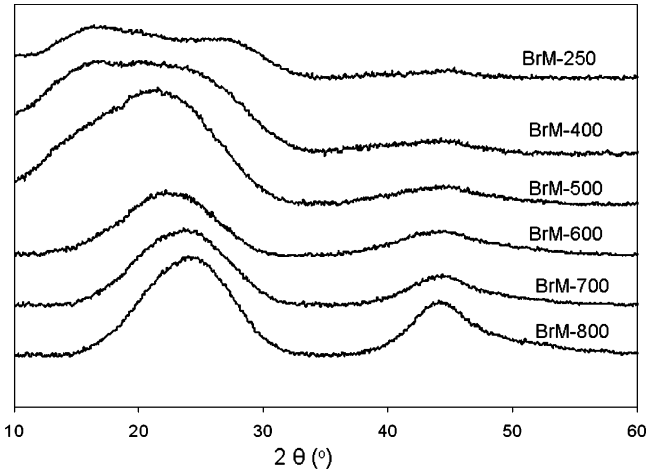

Figure 6. WAXD of carbon membranes from Br-Matrimid under different pyrolysis temperatures.

represents the repeated aromatic ring in graphitic structure. When the pyrolysis temperature reaches 800 °C, the peak position is near 25°, where *d*-spacing is 3.56 Å accordingly. This value is slightly greater than interlayer spacing, d_{002}, of graphite crystal. However, it still can be attributed to the average spacing between neighboring two hexagonal layers. Therefore, we can conclude that the monolayer graphite sheets should be formed in carbon membranes during high-temperature pyrolysis. Moreover the structure of carbon membranes can be described as turbostratic stacking of hexagonal layers and tends to approach graphitic crystal state with increasing temperature.

Compared with carbon membranes derived from the original Matrimid reported by Tin et al.,[18] the distance between hexagonal layers in carbon membranes derived from brominated Matrimid decreases from 3.68 to 3.56 Å. This indicates better crystallized graphite structures in carbon membranes when polyimide precursors were brominated before pyrolysis. In previous studies,[27,38−39] two fundamental conditions for obtaining well-crystallized graphite films were concluded: (1) flatness of the starting imide molecules; (2) high degree of orientation of these flat molecules along the film. As shown in Table 1, the molecular simulation indicates that the dihedral angle between the imide ring and the aromatic ring is ∼50.4° in both the unmodified and brominated Matrimid polyimide. This is due to the fact that the bromine is added on the phenyl ring of diamine parts, which seldom affects the flatness of the whole imide molecules. According to the report of Hasegawa et al.,[40] the degree of in-plane orientation is related to the polymer chain linearity, the interchain interaction, and the molecular chain mobility. From DSC and simulation results, bromination decreases polyimide chain flexibility, resulting in better chain linearity and higher degree of in-plane orientation of polyimide chains. Therefore, the better crystallized graphite structures in carbon membranes derived from brominated Matrimid could contribute to better orientation of polyimide chains along the film induced by bromine substitution. In addition, the formation of graphitic-like structure in carbon membranes at a high pyrolysis temperature could be considered as the reorganization of aromatic rings in the matrix. The formation and linkage of these aromatic rings by free radical reactions construct the graphitic planes. According to above discussion, the decomposition of brominated Matrimid may induce more free radicals in the system. Therefore, the bromination may promote the graphitization of carbon membranes.

3.3. Gas Permeation Analysis. The gas permeability and ideal selectivity of pure O_2, N_2, CO_2, and CH_4 through polyimides and their derived carbon membranes carbonized at 550 and 800 °C under vacuum environment are summarized in Table 2. As reported by Guiver et al., the increase in gas permeability of brominated Matrimid was attributed to the loosening of interchain packing by the bulky bromine group, which was shown by *d*-spacing measurement and FFV tests.[34]

Comparison between two carbon membranes derived from Matrimid and Br-Matrimid precursors shows that the gas permeability of carbon membranes from Br-Matrimid are obviously greater than those of carbon membranes from Matrimid when pyrolyzed at 550 °C. This result is consistent with Park et al.[22] and our previous findings[27] that the FFV of polymer precursors is an important factor to determine the performance of resultant carbon membranes pyrolyzed at a low temperature. It is expected that polymer precursors with a larger FFV will produce carbon membranes with a looser structure. In addition, there is another possible explanation for above phenomenon according to the results of TGA-FTIR. After bromination, Matrimid polyimide shows lower thermal stability. This implies that the Br-Matrimid emits more gaseous products than Matrimid at the same pyrolysis temperature. Since the opening structure of carbon membranes is mainly the

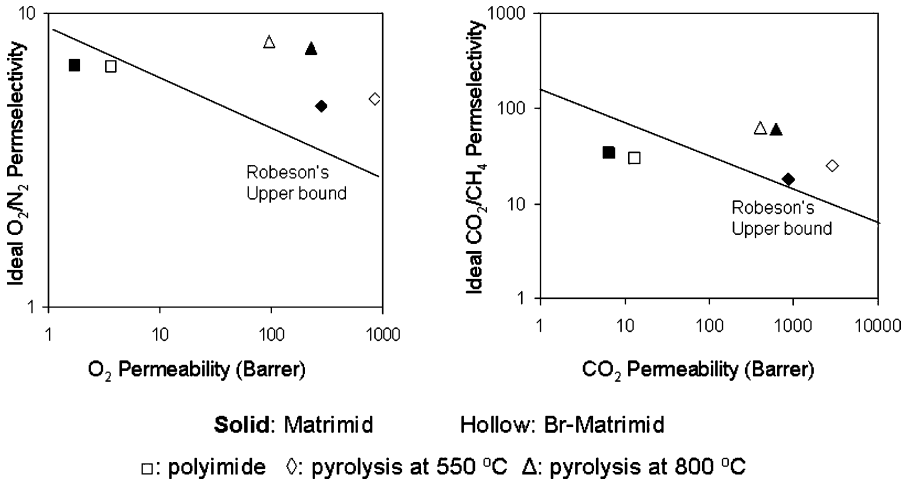

Figure 7. Gas permeability/permselectivity behavior with respect to the tradeoff lines for O_2/N_2 and CO_2/CH_4 gas pairs.

Table 2. Pure Gas Permeation through Polyimides and Their Derived Carbon Membranes

	permeability coefficient (barrers)					permselectivity		
	He	O_2	N_2	CH_4	CO_2	O_2/N_2	CO_2/CH_4	He/N_2
Br-Matrimid	38	3.6	0.55	0.44	13.3	6.5	30	69
Matrimid	21	1.7	0.25	0.19	6.5	6.6	34	84
CMs from Br-Matrimid (550 °C)	1960	850	168	116	2900	5.1	25	12
CMs from Matrimid (550 °C)	537	280	59	48	871	4.8	18	9.0
CMs from Br-Matrimid (800 °C)	290	96	12	6.4	402	8.0	63	24
CMs from Matrimid (800 °C)	403	227	30	10	611	7.6	61	13

result of the evaporation of gaseous products during the decomposition of polyimide, the Br-Matrimid which exhibits more weight loss during the pyrolysis process may create more interstitial space and result in having higher gas permeability. Interestingly, the gas selectivity of carbon membranes from Br-Matrimid is also higher than those of carbon membranes from unmodified Matrimid. Two kinds of pores, which are ultramicropore and micropore, may be formed in carbon membranes prepared at a low temperature. Generally, the dimension of ultra-micropore is close to the *d*-spacing of polyimide precursors (5−6 Å), while the size of micropores is larger than 10 Å. The gas selectivity is determined by the dimension and shape of ultramicropores. Thus, one of the possible reasons for the higher gas selectivity of carbon membranes derived from Br-Matrimid is that much greater interconnection between ultra-micropores formed by the evolution of decomposed products.

When the pyrolysis temperature is increased to 800 °C, the gas permeability of the resultant carbon membranes decreases as compared to those of carbon membranes pyrolyzed at 550 °C. Simultaneously, the selectivity of O_2/N_2 and CO_2/CH_4 improves after pyrolysis at higher temperatures. According to the WAXD results, high temperature pyrolysis results in the transformation of amorphous carbon materials to graphitic-like structure consisting of shrunken ultra-micropores. This suggests that the main mechanism involved in the gas transport through carbon membranes is molecular sieving, where the membranes can effectively discriminate gas molecules with similar molecular sizes. As compared to the selectivity of O_2/N_2, the degree of increment is higher for CO_2/CH_4, probably due to the greater difference in molecular sizes of CO_2/CH_4, since a higher pyrolysis temperature may result in a decrease in solubility selectivity of gases.[41] Interestingly, the gas permeability decrement of carbon membranes pyrolyzed from Br-Matrimid at 800 °C is much more significant than that of carbon membrane derived from unmodified Matrimid. As a consequence, unlike the carbon membranes pyrolyzed at a low temperature, the bromination resulted in the carbon membranes with lower permeability when pyrolyzing at a high temperature. As previously discussed, the better linearity and lower thermal stability of brominated polyimides induce a more ordered and better graphitic structure of resultant carbon membranes when the pyrolysis temperature increased to 800 °C. Carbon membranes with better graphitic structure possess less and narrower channels in which gas molecules can pass through. Therefore, the gas permeability of carbon membranes decreases when polyimide precursor is brominated before pyrolysis.

Figure 7 shows the tradeoff line between the selectivity and permeability for O_2/N_2 and CO_2/CH_4 pairs. It is clear that both permeability and selectivity of membranes are well above the upper-bound curve after carbonization. From their distance to the Robeson tradeoff line,[42] it is easy to visualize how much the performance of polyimide membranes can be improved when they are properly pyrolyzed. A comparison between gas separation performance of carbon membranes from unmodified Matrimid and Br-Matrimid indicates that the bromination of Matrimid precursor significantly improves the gas separation performance of resultant carbon membranes when a low pyrolysis temperature is used. At a high pyrolysis temperature, the improvement of gas separation performance is not so impressive by bromination, due to the tremendous decrease in the gas permeability of carbon membranes.

4. Conclusion

Commercial Matrimid polyimide was brominated before carbonization to increase the polymer chain rigidity and bulkiness. TGA-FTIR tests indicated that bromination not only increases the FFV of Matrimid polyimide but also decreases the thermal stability of Matrimid. It is shown that the addition of the bromine atoms onto Matrimid main chains significantly affects the pyrolysis behavior and the structure of resultant carbon membranes. As a result, bromination produces carbon membranes with higher gas permeability as compared to untreated carbon membranes. Furthermore, the permselectivity of modified carbon membrane remains competitive with unmodified carbon membranes. However, at pyrolysis temperatures of 800 °C, the gas permeabilities of carbon membranes from Br-Matrimid decrease to lower than that of carbon membranes from the original Matrimid. Molecular simulation shows that the bromination modification increases the linearity of polymer chains without changing the flatness of polymer molecules. Therefore, a more graphitic-like structure is obtained when brominated precursors are carbonized at a high temperature. In brief, bromination is a useful pretreatment for commercial polyimide precursors in improving the gas separation properties of carbon membranes when pyrolyzed at a low temperature.

Acknowledgment. This research was funded by the A*Star−NRC joint research program, which the authors gratefully acknowledge. The authors would also like to thank A*Star and NUS for funding this research with Grants R-279-000-113-304 and R-279-000-184-112, respectively. Special thanks are due to Ms. Pei Shi Tin and Ms. Mei Lin Chng for their useful help.

References and Notes

(1) Paul, D. R.; Yampol'skii, Y. P. *Polymeric Gas Separation Membranes*; CRC Press: Boca Raton, FL, 1994.

(2) Matsuura, T. *Synthetic Membranes and Membrane Separation Processes*; CRC Press: Boca Raton, FL, 1994.

(3) Ho, W. S. W.; Sirkar, K. K. *Membrane Handbook*, Ed.; Van Nostrand Reinhold: New York, 1992.

(4) Stern, S. A. *J. Membr. Sci.* **1994**, *94*, 1−65.

(5) Koros, W. J.; Mahajan, R. *J. Membr. Sci.* **2000**, *175*, 181−196.
(6) Saufi, S. M.; Ismail, A. F. *Carbon* **2004**, *42*, 241−259.
(7) Chen, Y. D.; Yang, R. T. *Ind. Eng. Chem. Res.* **1994**, *33*, 3146−3153.
(8) Rao, M. B.; Sircar, S.; Golden, C. US Patent 5104425, 1992.
(9) Centeno, T. A.; Fuertes, A. B. *Carbon* **2000**, *38*, 1067−1073.
(10) Koresh, J. E.; Soffer, A. *Sep. Sci. Technol.,* **1983**, *18*, 723−734.
(11) Soffer, A.; Azariah, M.; Amar, A.; Cohen, H.; Golub, D.; Saguee, S.; Tobias, H. US Patent 5695818, 1997.
(12) Centeno, T. A.; Fuertes, A. B. *J. Membr. Sci.* **1999**, *160*, 201−211.
(13) Zhou, W. L.; Yoshino, M.; Kita, H.; Okamoto, K. *Ind. Eng. Chem. Res.* **2001**, *40*, 4801−4807.
(14) Chen, J. C.; Harrison, I. R. *Carbon*, **2002**, *40*, 25−45.
(15) Sedigh, M. G.; Jahangiri, M.; Liu, P. K. T.; Sahimi, M.; Tsotsis, T. T. *AIChE J.* **2000**, *46*, 2245−2255.
(16) Fuertes, A. B.; Centeno, T. A. *Microporous Mesoporous Mater.* **1998**, *26*, 23−26.
(17) Fuertes, A. B.; Nevskaia, D. M.; Centeno, T. A. *Microporous Mesoporous Mater.* **1999**, *33*, 115−125.
(18) Tin, P. S.; Chung, T. S.; Hill, A. J. *Ind. Eng. Chem. Res.* **2004**, *43*, 6476−6483.
(19) Tin, P. S.; Chung, T. S.; Kawi, S.; Guiver, M. D. *Microporous Mesoporous Mater.* **2004**, *73*, 151−160.
(20) Tin, P. S.; Chung, T. S.; Liu, Y.; Wang, R. *Carbon* **2004**, *42*, 3123−3131.
(21) Singh, G. A.; Koros, W. J. *J. Membr. Sci.* **2000**, *174*, 177−188.
(22) Park, H. B.; Kim, Y. K.; Lee, J. M.; Lee, S. Y.; Lee, Y. M. *J. Membr. Sci.* **2004**, *229*, 117−127.
(23) Kim, Y. K.; Lee J. M.; Park, H. B.; Lee, Y. M. *J. Membr. Sci.* **2004**, *235*, 139−146.
(24) Jones, C. W.; Koros, W. J. *Carbon* **1994**, *32*, 1419−1425.
(25) Kusuki, Y.; Shimazaki, H.; Tanihara, N.; Nakanishi, S.; Toshinaga, T. *J. Membr. Sci.* **1997**, *134*, 245−253.
(26) Okamoto, K.; Kawamura, S.; Yoshino, M.; Kita, H.; Hirayama, Y.; Tanihara, N.; Kusuki, Y. *Ind. Eng. Chem. Res.* **1999**, *38*, 4424−4432.
(27) Xiao, Y.; Chung, T. S.; Chng, M. L.; Tamai, S.; Yamaguchi, A. *J. Phys. Chem. B* **2005**, *109*, 18741−18748.
(28) Geiszler, V. C.; Koros, W. J. *Ind. Eng. Chem. Res.* **1996**, *35*, 2999−3003.
(29) McCaig, M. S.; Seo, E. D.; Paul, D. R. *Polymer* **1999**, *40*, 3367−3382.
(30) Percec, S.; Li, G. *ACS Symp. Ser.* **1988,** *364*.
(31) Hamad, F.; Khulbe, K. C.; Matsuura, T. *Desalination* **2002**, *148*, 369−375.
(32) Okamoto, K. I.; Ijyuin, T.; Fujiwara, S.; Wang, H. *Polym. J.* **1998**, *30*, 492−498.
(33) Liou, G. S.; Wang, J. S. B.; Tseng, S. T.; Tsiang, R. C. C. *J. Polym. Sci., Part A: Polym. Chem.* **1999**, *37*, 1673−1680.
(34) Guiver, M. D.; Robertson, G. P.; Dai, Y.; Bilodeau, F.; Kang, Y. S.; Lee, K. J.; Jho, J. Y.; Won, J. *J. Polym. Sci., Part A: Polym. Chem.* **2002**, *40*, 4193−4204.
(35) Cerius^2 simulation tool user's reference, molecular simulations software for material science (Molecular Simulation Inc., San Diego, CA, 1996).
(36) Lin, W. H.; Vora, R. H.; Chung, T. S. *J. Polym. Sci., Part B: Polym. Phys.* **2000**, *38*, 2703−2713.
(37) Konno, H.; Nakahashi, T.; Inagaki, M. *Carbon* **1997**, *35*, 669−674.
(38) Hatori, H.; Yamada, Y.; Shiraishi, M. *Carbon* **1992**, *30*, 763−766.
(39) Inagaki, M.; Sato, M.; Takeichi, M.; Yoshida, A.; Hishiyama, Y. *Carbon* **1992**, *30*, 903−905.
(40) Hasegawa, M.; Matano, T.; Shindo. Y.; Sugimura, T. *Macromolecules* **1996**, *29*, 7897−7909.
(41) Suda, H.; Haraya, K. *J. Phys. Chem. B* **1997**, *101*, 3988−3994.
(42) Robeson, L. M. *J. Membr. Sci.* **1991**, *62*, 165−185.

MA051354J